RSC Advances




ROYAL SOCIETY OF CHEMISTRY

www.rsc.org/advances

RSC Advances

RSCPublishing

Paper

# Suppressing *Pseudomonas aeruginosa* Adhesion via Non-Fouling Polymer Brushes

Cite this: DOI: 10.1039/x0xx00000x

Received,
Accepted

DOI: 10.1039/x0xx00000x

www.rsc.org/

Cesar Rodriguez-Emmenegger,[1,2,3,*] Antje Decker,[4] František Surman,[1] Corinna M. Preuss,[2] Zdeňka Sedlákova,[1] Nicolas Zydziak,[2,3] Christopher Barner-Kowollik[2,3,*] Thomas Schwartz,[4] and Leonie Barner[3*]

In the current study, well-defined polymer brushes are shown as an effective surface modification to resist biofilm formation from opportunistic pathogens. Poly[oligo(ethylene glycol)methyl ether methacrylate] (poly(MeOEGMA)) and poly[*N*-(2-hydroxypropyl)methacrylamide] (poly(HPMA)) brushes were grown by surface initiated atom transfer radical polymerization (SI-ATRP) and subsequently characterized by Fourier-Transform infrared (FTIR) spectroscopy, X-ray photoelectron (XPS) spectroscopy and dynamic water contact angle measurements. Their remarkable resistance to protein fouling after long term contact with biological media was evidenced by surface plasmon resonance spectroscopy. Challenging these brushes with an environmental strain of *Pseudomonas aeruginosa* in mineral media as well as casein-soja-pepton-agar (CASO) medium resulted in no biofilm formation, while a decrease of the biofilm formation by 70% (poly(HPMA)) and 90% (poly(MeOEGMA)) was observed when the medium was rich in nutrients and proteins (fetal bovine serum). In contrast to the antibiotic sensitive strains, a biofilm formation was observed using an antibiotic multi-resistant *P. aeruginosa* strain on both brushes. Protein fouling was fully prevented on both type of brushes, which might challenge the proposed mechanism of biofilm formation mediated by a pre-formed conditioning film of proteins. The resistance to biofilm formation and the possibility to precisely control their growth and functionalities makes these brushes ((poly(HPMA) and (poly(MeOEGMA)) promising candidates for surface modification of various biomaterials as well as platforms for basic studies into the mechanisms of bacteria fouling.

## Introduction

Bacterial colonization of surfaces and interfaces has a major impact on various biotechnological areas. Some of the various detrimental effects include accelerated corrosion of metals (biocorrosion),[1] contamination of food causing food spoilage or posing serious risks to public health as well as infections and sepsis due to bacteria adhered to implants.[2-5] In particular, bacterial infection caused by implanted medical devices such as catheters and artificial prosthetics is a serious ongoing problem in the biomedical field. Of the 2.6 million orthopedic implants used annually only in the United States, approximately 110 000 (2-4.3%) led to hospital acquired (nosocomial) infections.[3, 4, 6, 7] Considering all implanted devices, the number of implant-related bacterial infections approaches 1 million per year.[8] An additional serious problem is that systemically administered antibiotics display constantly decreasing efficiency against implant-associated infections.[9] Approximately 70% of nosocomial infections are resistant to at least one antibiotic, and the trend is increasing leading to a constantly growing number of nosocomial infections with lethal outcome. The aforementioned implant-associated infections are caused by bacterial adhesion to the implant surface and subsequent formation of bacterial biofilms.[10] A biofilm is a matrix on a solid surface harboring microorganisms aggregated by excreted extracellular polymeric substances (EPS).[11] Microbial biofilms represent a special symbiotic form of bacterial life that can be established on most natural and synthetic surfaces. The bacteria in a biofilm can be several orders of magnitude more resistant to antibiotic treatment than their planktonic counterparts, thus biofilms are typically very difficult to eradicate.[12, 13] They are also extremely resistant to both the immune response and thus their development is the primary cause of implant-associated infections.[8] Further, advances in life sciences and medicine

enable access to implantable biomaterials such as catheters, prosthesis, stents, and pacemakers to an increasing number of patients, and as a result a concomitant increase in the number of biofilm related infections is expected. Consequently, preventing bacterial adhesion and biofilm formation efficiently and permanently prior to implantation is of first importance to significantly reduce the risk of serious postoperative infections.

The extraordinary resistance of biofilms to conventional antibiotic therapy and its detrimental consequences have driven research into the development of novel surfaces and coatings able to prevent biofilm formation.[9, 14] It has been postulated that development of biofilms occurs in several steps: (i) the formation of a conditioning film either from components of the medium in contact with the surface or by the EPS generated by the bacteria, (ii) subsequent transport of the bacteria towards the substrate and (iii) adhesion. Hydrophobic surfaces in contact with protein-rich liquids suffer from a rapid fouling from proteins[15-17] which promotes the adhesion of bacteria by lowering the interfacial energy. Bacterial adhesion onto hydrophilic surfaces is a more complex process which is governed by specific receptor-ligand interactions (adhesins) as well as more general physicochemical interactions.[18] Initial adhesion is through long-range interactions, operating over distances of several tens of nanometers between bacterium and substrate, after which short-range interactions play a central role. Simplified models based on the Derjaguin-Landau-Verwey-Overbeek (DLVO) colloid theory have been proposed to understand these long-range interactions as well as considering the molecular conformation of the polymers on the coating.[19, 20] The driving forces of the interaction are the Liftshitz-Van der Waals forces and forces resulting from overlap of the electrical double layers[21-27] as modelled on weakly resistant poly(ethylene oxide) grafted-to chains.[27] Short-range interactions (hydrogen bonding, electrostatic, hydrophobic effects), on the other hand, strongly depend on the physicochemical properties of the surface. Once bacteria are attached to the surface, the transcription of specific genes is activated, resulting in the synthesis of EPS that encase the bacteria giving mechanical support and chemical resistance. Since the removal of the established biofilm cannot be readily accomplished, biofilm formation on the surface must be prevented by appropriate surface modification strongly limiting the contact of the substrate with live bacteria.

Two types of antibacterial coating have been developed based on (a) inactivating any bacterium which comes into contact with the surface (bactericidal coating) and (b) by generating an entropic barrier repelling the bacteria (antifouling). The bactericidal surfaces contain molecules, polymers or nanoparticles which are toxic for the bacteria. Typical examples include antibiotics, silver nanoparticles, quaternary ammonium compounds, cationic polymers, chitosan, and *N*-halamines among others. [22, 48, 49, 5, 28-32] However, their use is discouraged for biomedical applications due to their intrinsic cytotoxicity, especially in long-term applications. In addition, after the bacterium is inactivated on the surface it is often adsorbed modifying the surface properties and promoting the subsequent adhesion of new bacteria on top. To circumvent this phenomenon, switchable polymer brushes were introduced for antifouling surfaces. These brushes were grown as a poly(cation), which after killing the bacteria could be hydrolyzed to form an antifouling poly(carboxybetaine).[33] Regrettably, the switch was not reversible as it involved a hydrolysis step, thus presumably this surface modification can only resist the first bacteria which approach. In light of the intrinsic drawbacks of bactericidal coatings, the most promising strategy is to prevent bacterial adhesion (antifouling surfaces). The adhesion can be prevented by minimizing the forces driving the bacterium into contact with the substrate. For the coating to be effective, no primary nor secondary adsorption can be allowed, *i.e.* the coating should be homogeneous without pin-holes enabling direct contact with the substrate.[34-36] Further, the forces predicted by the DLVO theory should be minimized, *i.e.* by creation of a water barrier without a net charge and the introduction of steric hindrance to keep the bacteria at a distance from the surface, where long-range attractive interactions are at a minimum. In this context, poly(ethylene glycol) (PEG) as well as self-assembled monolayers of oligo(ethylene glycol) alkane thiols have been extensively utilized as antifouling films.[2, 37] Although PEG has been proposed as an ideal candidate to resist the biofilm formation, only a reduction of biofilms was achieved.[38, 39] Grafting PEG to a surface typically leads to thicknesses between 1 and 10 nm, which presumably does not lead to an effective sterical barrier.[27, 34, 35, 40, 41] In addition, end-grafted PEG has been shown to not resist the adsorbed proteins present in complex biological media which could facilitate the formation of a conditioning film facilitating colonization.[15, 17, 42] More recently, attention has been placed on mimicking natural superhydrophobic and self-cleaning surfaces (lotus leaves, gecko foot, shark skin and insect wings) to reduce the fouling, however, only limited success was achieved.[5] Arguably, the most versatile systems for the preparation of ultra-thin coatings are polymer brushes grown from the surface of the substrate. With the advent of surface initiated reversible deactivated radical polymerizations, such as atom transfer radical polymerization (ATRP),[43] reversible addition fragmentation transfer (RAFT) polymerization,[44] and single electron transfer radical polymerization (SET-LRP),[45] it has been possible to precisely engineer the properties of biointerfaces. These techniques combined with orthogonal ligation protocols for patterning enabled the preparation of mono, diblocks, and functional biointerfaces for various applications including bioactive paper and biosensors.[45] Polymer brushes of oligo(ethylene glycol) methacrylate, carboxybetaines and *N*-(2-hydroxy propyl)methacrylamide have shown an unmatched resistant to human blood plasma and other biofluids with which an implant could come into contact.[15, 46]

Despite the growing research in the field of antibacterial surfaces as well as biofilm biology, surfaces with long term resistance to biofilm formation remains elusive. In the current work, we evaluate the resistance to the formation of biofilm from laboratory and environmental strains of *Pseudomonas*



 

*aeruginosa* (*P. aeruginosa*) on two ultra-low fouling polymer brushes, poly[oligo(ethylene glycol)methyl ether methacrylate] (poly(MeOEGMA)) and poly[*N*-(2-hydroxypropyl)methacryl amide] (poly(HPMA)). *P. aeruginosa* is one of the most common opportunistic pathogens causing nosocomial infections.[47] In particular, its ability to rapidly form a stable biofilm makes it a very interesting model organism.[48] By studying the biofilm formation after exposing the surfaces to bacteria in media rich of proteins or without proteins, we assessed the links between protein fouling (determined by surface plasmon resonance spectroscopy, SPR) and the formation of a conditioning film that could enhance bacterial attachment.

## Experimental

### Materials

Oligo(ethylene glycol) methyl ether methacrylate ($M_n$ = 300 g·mol$^{-1}$, MeOEGMA), CuCl (99.999%), CuBr (99.999%), $CuBr_2$ (99.999%), 2,2'-dipyridyl (BiPy), 1,4,8,11-tetramethyl-1,4,8,11-tetraazacyclotetradecane ($Me_4$Cyclam), methacryloyl chloride, 1-aminopropan-2-ol, sodium carbonate, α-bromoisobutyryl bromide, and 11-mercapto-1-undecanol were purchased from Sigma-Aldrich. Phosphate buffered saline (PBS, 140 mM NaCl, 10 mM $Na_2HPO_4$, 2.7 mM KCl, 1.8 mM $KH_2PO_4$) was freshly prepared and adjusted to pH 7.4. CASO bouillon with peptone from casein (1.7%), peptone from soja beans (0.3%), NaCl (0.5%), $K_2HPO_4$ (0.25%), glucose-monohydrate (0.25 %), pH 7.3; BM2 mineral medium consisting of 7 mM $(NH_4)_2SO_4$, 40 mM $K_2HPO_4$, 22 mM $KH_2PO_4$, 0.4% glucose, 2 mM $MgSO_4$, 0.01 mM $FeSO_4$, pH 7.0; M9-medium consisting of 42 mM $Na_2HPO_4$, 22 mM $KH_2PO_4$, 8.6 mM NaCl, 18.7 mM $NH_4Cl$, 0,4% glucose, 1 mM $MgSO_4$, 0.1 mM $CaCl_2$, pH 7.0; and DMEM, with 10% Fetal Bovine Serum (FBS) were from SIGMA. The ATRP initiator ω-mercaptoundecyl bromoisobutyrate was synthesized by reacting α-bromoisobutyryl bromide with 11-mercapto-1-undecanol according to the method published earlier.[49] *N*-(2-hydroxypropyl) methacrylamide (HPMA) was synthesized according to literature procedures.[16] The inhibitor present in the macromonomer MeOEGMA (900 ppm of hydroquinone monomethyl ether) was removed by passing through a basic alumina column immediately before the polymerization experiment. All other chemical reagents were used without further purification. Blood plasma was kindly provided by the Institute of Hematology and Blood Transfusion, Prague, Czech Republic. The substrates were glass microscope slides (Waldermar Knittel) and silicon wafers (ON semiconductors, Czech Republic). Gold coated surfaces were prepared by evaporation of a titanium adhesion layer (3 nm) and subsequent evaporation of gold; 50 nm for chips for surface plasmon resonance (SPR) and coupons for bacterial culture, as well as 200 nm for the Si wafers for ellipsometry experiments.

### Surface preparation

**Self-assembled monolayer of initiator.** Gold-coated glass slides (SPR chips, coupons for bacteria adhesion studies) and gold-coated Si-wafer chips (for ellipsometry) were cleaned by rinsing twice with ethanol and deionized water, blow-dried with nitrogen, and cleaned in a UV/Ozone cleaner (Jelight) for 20 min. Immediately after cleaning, the chips were immersed in a 1 mM solution of ω-mercaptoundecyl bromoisobutyrate in ethanol and kept overnight in the dark at ambient temperature.

**Poly(MeOEGMA) brushes.** $CuBr_2$ (83.8 mg, 375 μmol), CuBr (269 mg, 1.86 mmol) and 2,2'-dipyridyl (774 mg, 4.96 mmol) were added to a one-neck Schlenk tube equipped with a magnetic stirring bar. The flask was evacuated and backfilled with argon followed by addition of 25 mL of previously degassed (*via* six freeze-pump-thaw cycles) methanol. In a second Schlenk flask, a solution of MeOEGMA (28.4 g, 94.8 mmol) in 25 mL of water was prepared and degassed using argon bubbling for 40 min in an ice bath. After full dissolution of the catalyst, the monomer solution was transferred to the catalyst solution using a gastight syringe. Subsequently, the homogenized polymerization mixture was transferred by cannula under argon atmosphere to the reactors containing the substrates with SAM of initiator. The polymerization was carried out at 30 °C for 50 min.[16, 50] The samples were taken out of the reactor, washed successively with ethanol and water and stored in milli-Q water.

**Poly(HPMA) brushes.** Methanol (44 mL) was degassed *via* six freeze-pump-thaw cycles and subsequently transferred under argon atmosphere to a Schlenk tube containing CuCl (116.3 mg, 1.18 mmol), $CuCl_2$ (35.4 mg, 263 μmol) and $Me_4$Cyclam (401 mg, 1.56 mmol). In a second Schlenk tube, the monomer HPMA (9.2 g, 64.2 mmol) was dissolved in 44 mL of previously degassed (*via* six freeze-pump-thaw cycles) water. The monomer solution was transferred to the blue catalyst solution using a gastight syringe. The homogenized polymerization mixture was transferred by cannula under argon atmosphere to the reactors containing the substrates with the SAM of the initiator. The polymerization was carried out at 30 °C for 2 h.[16] The samples were taken out of the reactor, washed successively with ethanol and water and stored in milli-Q water.

### Physicochemical characterization

**Ellipsometry.** The dry thickness of the layer was measured with a Spectroscopic Imaging Auto-Nulling Ellipsometer EP$^3$-SE (Nanofilm Technologies GmbH, Germany). The silicon substrates used for ellipsometry measurements were coated with a thicker gold layer (approx. 200 nm) than the SPR chips or coupons (used for biofilm studies), which permitted modelling it as bulk gold. Immediately prior to measurement, the brushes were blow-dried with nitrogen. The spectra were acquired in air at ambient temperature in the wavelength range of λ =399 to 811 nm at an angle of incidence (AOI) = 70º. The fitting was performed with the EP$^3$-SE, and the polymer layers

were modeled using a Cauchy dispersion function. Each chip was measured in three spots to confirm sample uniformity.

**X-Ray Photoelectron Spectroscopy (XPS).** The measurements were performed using a K-Alpha XPS spectrometer (ThermoFisher Scientific, East Grinstead, UK). All the samples were analyzed using a microfocused, monochromated Al Kα X-ray source (400 µm spot size). The kinetic energy of the electrons was measured by a 180º hemispherical energy analyzer operated in the constant analyzer energy mode (CAE) at 50 eV pass energy for elemental spectra. Data acquisition and processing using the Thermo Advantage software is described elsewhere.[51] The spectra were fitted with one or more Voigt profiles (binding energy uncertainty: +/- 0.2 eV). The analyzer transmission function, Scofield sensitivity factors,[52] and effective attenuation lengths (EALs) for photoelectrons were applied for quantification. EALs were calculated using the standard TPP-2M formalism.[53] All spectra were referenced to the C1s peak of hydrocarbons at 285.0 eV binding energy controlled by means of the well-known photoelectron peaks of metallic Cu, Ag, and Au.

**FTIR GASR spectroscopy.** Fourier-Transform Infrared Grazing Angle Specular Reflection (FTIR-GASR) spectra were obtained from the dry polymer brushes on gold-coated SPR chips using a Nicolet Nexus 870 FTIR spectrometer equipped with a SAGA GASR attachment (ThermoFisher Scientific) under continuous purging with dry air. The spectra were collected at 256 scans with 2 $cm^{-1}$ resolution with an aperture size of 16 mm.

**Dynamic water contact angle.** The dynamic sessile drop method was used to measure the water contact angle of the surfaces and to assess their wettability, with a DataPhysics OCA 20 instrument. A 5 µL drop was placed on the surface and its image was recorded as a video while the volume was increased up to 15 µL and decreased at a flow rate of 0.5 $\mu L \cdot s^{-1}$. The drop profile was fitted with a circular fitting algorithm to obtain the advancing and receding contact angles.

### Bacteria culture

**Bacteria and growth conditions.** Three strains of *P. aeruginosa*, PA30, PA49 and PA01, which differ in the origin of isolation, were used for the biofilm experiments. The PA01 is a laboratory reference strain, where the entire genome is already sequenced.[54] The other two strains were isolated from the sewers close to a surgery department in a German city. Commercial API 20NE (BioMérieux, Nürtingen, Germany) was used for the taxonomic identification. The resistance of the *Pseudomonas* isolates (Table 1) to gentamicine, ciprofloxacin, imipenem, ceftazidime, amikacin, azlocillin, and piperacillin/tazobactam was determined by antibiogram testing according to Performance Standards for Antimicrobial Susceptibility Testing; M100-S17, Clinical and Laboratory Standards Institute, (Wayne, PA). The zone of inhibition was measured after 18 h of incubation at 37 ºC.

**Table 1**. Agar diffusion resistance to antibiotics of *P. aeruginosa* isolates

| Isolate number | GM | CIP | IPM | CAZ | AN | AZ | PT |
|---|---|---|---|---|---|---|---|
| PA 49 | R | R | R | R | R | R | R |
| PA 30 | S | S | S | S | S | S | S |
| PA 01 | S | S | S | S | S | S | S |

Conditions of agar diffusion test: gentamicin (GM, 10 µg), ciprofloxacin (CIP, 5 µg), imipenem (IPM, 10 µg), ceftazidim (CAZ, 10 µg), amikacin (AN, 20 µg), azlocillin (AZ, 30 µg), and piperacillin/tazobactame (PT, 30/10 µg) resistance; S: susceptible; R: resistant.[55] (Data for PA 49 and PA 30 from Ref. [55].)

The three *P. aeruginosa* strains were cultivated in CASO broth (Carl Roth Ltd., Karlsruhe, Germany) overnight. The cells were precipitated and washed with PBS, and resuspended in the preferred media for subsequent biofilm analyses. The cell densities were adjusted to $1\times10^2$ colony forming units (CFU) per mL in accordance to Patenge *et al*.[56] For biofilm experiments, control and polymer coated substrates were exposed to different media with bacteria: (1) CASO; (2) BM2 mineral medium; (3) M9-medium; and (4) DMEM with 10% FBS.

### Resistance to fouling

**Surface plasmon resonance (SPR).** Protein fouling was studied using a custom-built SPR instrument (Institute of Photonics and Electronics, Academy of Sciences of the Czech Republic, Prague) based on the Kretschmann geometry of the attenuated total reflection method and spectral interrogation of the SPR conditions. Broadband light from a halogen lamp (Mikropack) was collimated, polarized coupled with the SPR sensing element using a prism. The SPR chip consists of a glass coated with an adhesion promoting titanium film (thickness 2 nm) and a gold film (thickness 50 nm) which is interfaced with the prism using a Cargille matching oil ($n_D$ = 1.5150±0.0002). Upon the incidence on the gold film, the light beam excites surface plasmons at a wavelength of 750 nm on four independent sensing spots. The reflected light is collected into four optical fibers and coupled to the spectrophotometer. The acquired spectra were analyzed in-real time enabling the independent determination of the resonant wavelength for each sensing channel. The refractive index resolution was $3\cdot10^{-7}$ RIU. A low volume (1 µL) flow-cell with four separate chambers facing each of the sensing spots was used. The sensor was equipped with a temperature controller which enables to stabilize the temperature in a range of 0.01 ºC. The tested solutions were driven for 15 min or 10 h at 25 $\mu L \cdot min^{-1}$ by a peristaltic pump through four independent channels of a flow cell in which SPR responses were measured simultaneously. PBS was flown until a stable baseline was achieved (approximately 15 min). Subsequently, it was replaced by the samples (FBS 10% in PBS or HS, 10% in PBS) to be tested for 15 min or 10 h and then replaced once again with PBS. The sensor response ($\Delta\lambda_{res}$) was obtained by the difference between the baselines in PBS before and after the injection of the tested samples. The sensor response can be calibrated to the mass deposited at the surface of bound molecules. A shift of $\Delta\lambda_{res}$ =



 

1 nm corresponds to a change in the deposited protein mass of 150 pg·mm$^{-2}$.[57] The LOD was estimated as the sensor response equivalent to 3 standard deviations of the baseline noise (0.02 nm, equivalent to 0.3 ng·cm$^{-2}$.

**Bacterial adhesion assay.** The coupons (26×16×1 mm$^3$) used as substrates for biofilm analyses were put in the holder of the custom-made biofilm reactors. The size of the biofilm reactor was 290 mm in length, 46 mm inner diameter with a liquid capacity of 450 mL in maximum. The flow through rate of the different media was 2 L·d$^{-1}$. Two control coupons (SAM), two HPMA modified coupons, and two MeOEGMA modified coupons were fitted in one holder for each biofilm experiment. The assemblies of the biofilm reactors were carried out in presence of PBS or media to avoid long term air exposure of the modified surfaces. When the reactor assembly was finished, the system was inoculated with bacteria suspensions containing 1x10$^2$ CFU·mL$^{-1}$. The coupons were positioned vertically to avoid any sedimentation of bacteria during the experiment. The bacteria inocula were circulated for max. 12 h overnight to induce initial adhesion processes. Subsequently, sterile media ran through the biofilm reactors with a flow rate of 2 L·d$^{-1}$.

**Fluorescence staining and quantification of biofilm formation.** Staining of biofilms was performed at the end of the experiments (7 d) according to manufacturer's instructions using Living/Dead BacLight Viability Kit (Invitrogen Karlsruhe, Germany). Briefly, planktonic cells were removed by a washing step using PBS and the remaining biofilms were simultaneously stained with 5 µM SYTO9 and 15 µM propidium iodide for 15 min. Residual dye solutions were removed by washing with buffer solution. Images were acquired using an Axioplan2 imaging system (Zeiss, Oberkochen, Germany) at 100-fold magnification. Digital images were recorded at same light intensities with a Zeiss AxioCamMRm camera and AxioVision 4.6 software. For correlation experiments the acquired images were analyzed by their fluorescence intensities (green fluorescence for living bacteria and red fluorescence for dead bacteria) using ImageJ software (Comstat2-Plugin). A number of five different microscopic visual fields from each substrate sample were analyzed to quantify the biofilm coverage.

## Results and discussions

In the current study, the adhesion of different strains of *P. aeruginosa* and the formation of biofilms on highly protein resistant polymer brushes, poly(MeOEGMA) and poly(HPMA), was assessed. Firstly, a SAM of ω-mercaptoundecyl bromoisobutyrate on gold coated substrates was prepared which was subsequently utilized as initiating sites for the grafting of HPMA and MeOEGMA *via* SI-ATRP. Poly(MeOEGMA) stands as one of the most versatile polymer brushes for antifouling properties. The SI-ATRP of this monomer has been shown to be well controlled in water, buffers and even biological fluids as evidenced by the linear evolution of thickness with time as well as for being susceptible to block copolymer formation.[42, 58, 59]

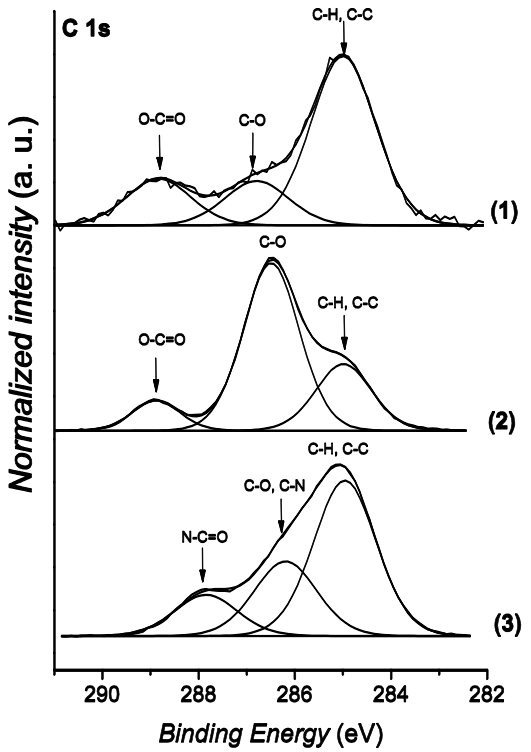


**Figure 1.** XPS C1s core level spectra of the studied surfaces: (1) SAM, (2) poly(MeOEGMA) and (3) poly(HPMA) brushes.

The excellent control during ATRP is achieved by using a combination of Cu(I) and Cu(II) leading to rapid ATRP equilibrium thus enabling to precisely design the properties of the surface. The SI-ATRP of HPMA shows the typical drawbacks of (meth)acrylamide monomers, however – as demonstrated previously – by changing the polymerization conditions various thicknesses can be precisely accessed.[16] The prepared brushes resulted in continuous films free of in-holes with a very low root mean square roughness as shown in Figure S7 via AFM. Remarkably, poly(HPMA) has shown unmatched resistance to blood plasma fouling (undetectable) even after 2 years storage.[16] The polymerizations accounted for polymer brushes with a thickness of 30 nm (Table 2).

**Table 2.** Thickness and wettability determined as dynamic water contact angles of the tested surfaces

| Surface | Ellipsometric thickness (nm) | Dynamic water contact angles | |
|---|---|---|---|
| | | $\Theta_{adv}$ (°) | $\Theta_{rec}$ (°) |
| Gold | - | 76.2 ± 0.9 | 63.3 ± 0.5 |
| SAM initiator | 1.4 ± 0.3 | 62.3 ± 0.7 | 45.1 ± 1.3 |
| Poly(MeOEGMA) | 30.7 ± 0.4 | 43.9 ± 0.6 | 23.8 ± 0.3 |
| Poly(HPMA) | 29.8 ± 0.6 | 40.3 ± 0.2 | 21.5 ± 0.6 |

Comparison of C1s XPS spectra (Figure 1) of the SAM and poly(MeOEGMA) shows a strong increase of the peaks assigned to [C-O] bonds at 286.4 eV, stemming from oligo(ethylene glycol) side chains of the brush and a decrease

of the signal corresponding to [C-H, C-C] at 285.0 eV, proving the successful polymerization.[50] Inspection of the FTIR GASR spectra displays bands at 1730 $cm^{-1}$ (ester carbonyl), 1465 $cm^{-1}$ ($CH_2$ scissoring), 1350 $cm^{-1}$ ($CH_2$ wagging), 1250 $cm^{-1}$ ($CH_2$ twisting), 950 $cm^{-1}$ ($CH_2$ rocking) and a prominent band at 1145 $cm^{-1}$ (C-O-C stretching), thus further confirming the successful grafting of poly(MeOEGMA) brushes (Figure S1, (2)).

XPS analysis of poly(HPMA) brushes shows signals assigned to [N-C=O] and [C-N] at 287.9 and 286.5 eV characteristic of amide polymers. The experimental atomic ratios [C-C, C-H]:[C-O, C-N]:[C=O] = 4:2:1 closely match the theoretical values. In addition, the integral of the nitrogen signal assigned to the amide band (400.0 eV) in the N1s spectrum equals the one found in the C1s spectrum at 287.9 eV.[60] Further evidence of the successful grafting of poly(HPMA) was obtained from FTIR-GASR spectrum (see Figure S1, (3)) clearly showing the amide I and II bands at 1650 and 1540 $cm^{-1}$.[16]

A low surface energy and high wettability has been proposed as one of the mechanisms behind resistance to fouling.[61] A high wettability gives rise to an enthalpic barrier as water molecules have to be removed for proteins or bacteria to foul the surface.[62] Both surface modifications increased the wettability of the surfaces as evidenced by the decrease in the water contact angles. The larger differences between the SAM and the brushes was observed in the receding contact angles ($\Theta_{rec}$); 45.1, 23.8 and 21.5º for SAM, poly(MeOEGMA) and poly(HPMA) respectively (Table 2). The $\Theta_{rec}$ are more representative values of the conditions that the surfaces will meet during their use when interfacing with the hydrated biological milieu.

**Protein fouling**

Exposure of the presented surfaces to complex biological media emulating the condition of the present work (10% FBS) and even of more fouling media such as human serum (HS) was performed to investigate whether the fouling leading to the formation of a conditioning film could enhance bacterial attachment. Arguably, such type of conditioning film develop in most medical devices coming into contact with biological fluids and has been proposed to promote initial bacterial attachment. [63] Thus the resistance to fouling of the surfaces to human serum (10% in PBS, HS) and fetal bovine serum (10% in PBS, FBS) using surface plasmon resonance (SPR) was examined. The samples were challenged with the protein mixtures HS and FBS (10%) for 15 min and 10 h. After 15 min contact, no fouling from HS nor FBS was detected on poly(HPMA) (refer to Table S1, and Figure S2 and S3, ESI) in agreement with our previous reports.[15, 16] Only a very low fouling (87 and 78 $pg \cdot mm^{-2}$ for FBS and HS) was observed after 10 h exposure, which is equivalent to less than 3% of a monolayer of proteins. Similar results were achieved on poly(MeOEGMA) brushes, displaying undetectable fouling for FBS (LOD of SPR 3 $pg \cdot mm^{-2}$), whereas 43 and 584 $pg \cdot mm^{-2}$ were observed after 15 min and 10 h contact with HS (Table S1, ESI). To rule out any concentration effect, the fouling from undiluted human serum and undiluted FBS were also assessed, leading to analogous results (ESI, S4 and S5).The extremely low fouling from FBS indicates that no conditioning film forms under the studied conditions, rendering these polymer brushes excellent candidates to suppress fouling from bacteria.

**Bacterial adhesion**

Prevention of bacterial adhesion is of central importance in medicine. Therefore, the adhesion of two environmental strains and a reference strain in 4 different media onto the poly(MeOEGMA) and poly(HPMA) brushes was investigated. The surfaces were placed in a plug-flow biofilm reactor in which the bacteria suspension were continuously pumped through at a controlled temperature. The cultures were used to start the biofilm cultivation on the coupons coated with poly(MeOEGMA) and poly(HPMA) antifouling brushes and their SAM as a control. The hydrophobicity of the SAM of initiator accounts for a realistic model of a large number of polymeric surfaces which may come into contact with bacteria. To assess the long term repulsive properties of the surface modifications the contact time was set to 7 days, during which sterile media continuously run through the biofilm reactor after the inoculation phase. Growth curves in close systems showed that the three strains display similar growth rates (Figure S6, ESI). To quantify the bacteria adhesion and biofilm formation, the surfaces were stained with LIVE/DEAD *Bac*Light Kit and analyzed by fluorescence microscopy. The intensity per unit area was utilized to quantify the coverage of the surface.

Firstly, it was confirmed that the staining agent did not bind to the brushes in a large extent which could impair the characterization. The coupons were stained using the same protocol as for the samples in contact with *P. aeruginosa*, obtaining fluorescence intensities of 5.7±2.5, 2.3±1.1 and 2.6±0.6 $mm^{-2}$ for the SAM, poly(HPMA) and poly(MeOEGMA) surfaces. These low values, close to the standard deviation, do not interfere with the quantification of the biofilm formation. Thus, this methodology can be used to assess the extent of biofilm coverage on the surfaces.

Figure 2 depicts the fluorescence micrographs of the tested surfaces after 7 days contact with an environmental strain, PA30, in 4 different media. The fouling observed on mineral media M9 and BM2 is very low, even on SAMs, and below or very close to the control signal for both polymer brushes. Even if various publications have focused their attention on similar media, the lack of nutrients as well as of proteins (which could form a conditioning film that results in very poor biofilm formation on any surface) requires that more challenging media need to be assessed to mimic real applications.[55, 64, 65] Examination of *P. aeruginosa* adhesion on SAM-coated coupons reveals a much higher biofilm formation on nutrient rich media, *i.e.* CASO and 10% FBS, than in the mineral media M9 and BM2 (Figure 3, (1) and (2)). This observation is in agreement with previous reports.[55] It is accepted that the settlement, adhesion and proliferation of bacteria is promoted and enhanced by the formation of a protein film. The SAMs as well as the surfaces of most biomedical equipment interfacing



 

biological media are rapidly fouled by protein containing solutions as we have previously shown.[15-17, 59]

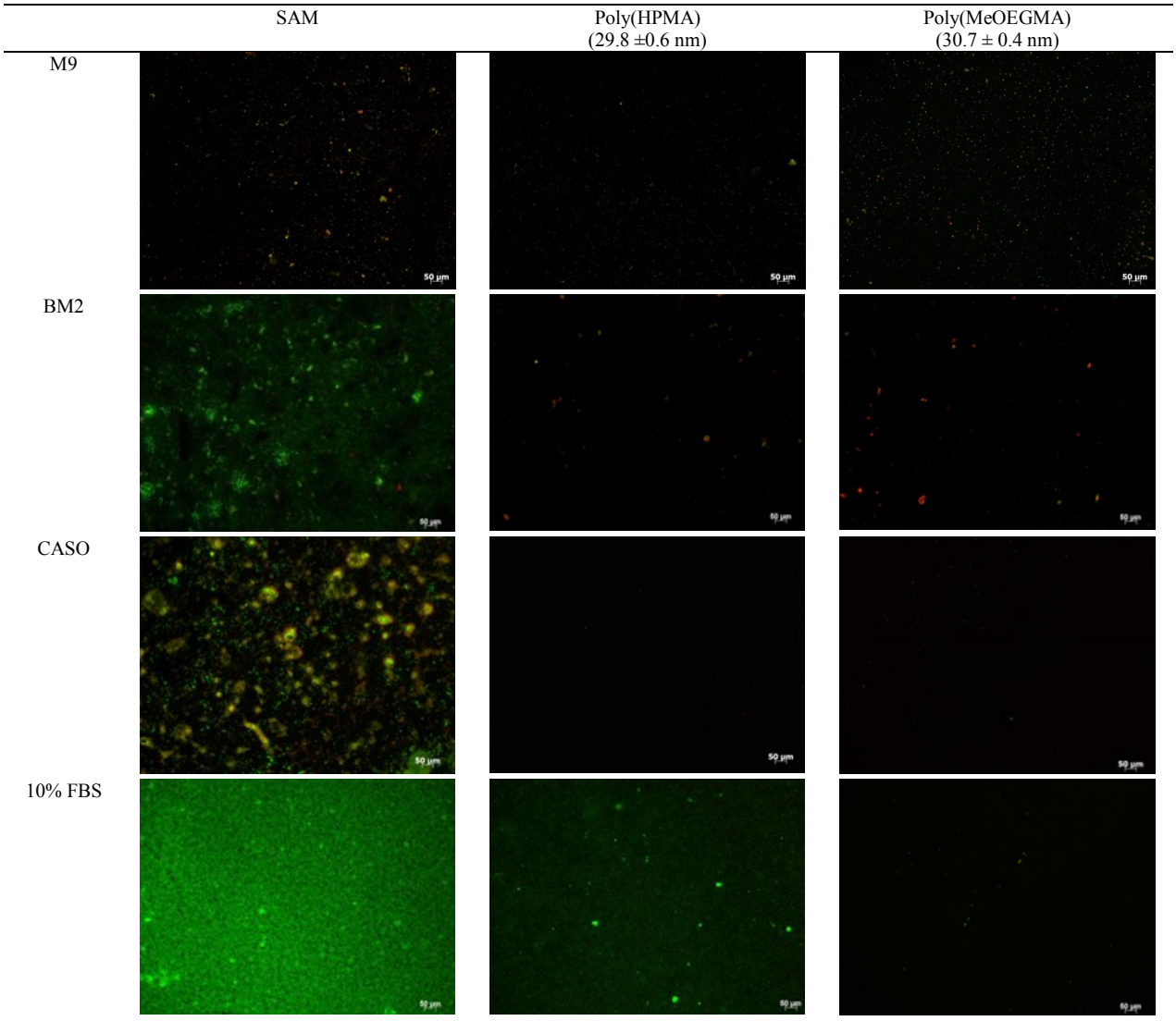


**Figure 2**. Fluorescence micrographs of biofilms on SAM, Poly(HPMA), and Poly(MeOEGMA) surfaces after 7 days surface exposure to the environmental strain of *P. aeruginosa* (PA30) in different media (M9, BM2, CASO and 10% FBS). Scale bar 50 µm. Surfaces were stained with a LIVE/DEAD BacLight Kit.

While massive biofilm coverage was observed in the SAM in contact with CASO or 10% FBS, much lower coverage was observed on the polymer brushes which prevent protein fouling. The fluorescence intensity on both brush surfaces ($1.9\pm0.4$ mm$^{-2}$ for poly(HPMA) and $1.5\pm0.6$ mm$^{-2}$ for poly(MeOEGMA)) after contact with PA30 in CASO was well below the fluorescence observed on their controls (Figure 3). While most reported studies have been carried out in CASO or mineral media, 10% FBS poses a much higher challenge to the surfaces. The fouling observed on the SAM after 7 days in 10% FBS was 8.4 times higher than the one observed on the SAM using bacteria suspension in M9 and 3.3 times higher than the one observed in CASO. On the other hand, poly(HPMA) and poly(MeOEGMA) brushes decreased the fouling from the environmental strain, PA30, by 70 and 90% compared to SAM (Figure 2 and 3). The remarkable resistance of both brushes is in line with their ability to prevent protein fouling from complex biological media.[15, 16, 59] Protein deposits resulting in a film are ubiquitous to most (bio)materials interfacing biological media and result in an attractive surface for bacteria colonization. Thus, surfaces preventing protein fouling are a prerequisite for prevention of bacterial biofilm formation.

The fluorescence staining with Syto9 and propidium iodide (LIVE/DEAD BacLight Kit) for live-dead discrimination of biofilm bacteria demonstrated a high percentage of living (*i.e.* green fluorescent) bacteria in biofilms grown on SAM control

materials. This became most evident during biofilm experiments with high nutrient media (see Figure 2, CASO and 10% FBS). In case of surfaces coated with polymer most of the residual bacteria appeared to be dead (red fluorescent), indicating a passive attachment of already dead or injured cells only. It is worth noticing, that the demonstrated strong anchoring of the brushes to gold[16] indicates that the presence of dead bacteria could not be caused by leaching of polymer chains to the surrounding media.

**Biofilm formation of different strains of *P. aureginosa***

*P. aeruginosa* is known to have very high genotypic variability and a concomitant flexibility in growth, biofilm formation and capacity to adapt to adverse conditions. Thus, we tested a reference strain (PA01) and another antibiotic multi-resistant environmental strain (PA49). Examination of the fouling from PA01 (Figure 3, (2)) clearly indicates similar trends than for PA30. Very low fouling – only single cells or microcolonies – were observed on the brushes when the bacteria were suspended in the mineral media. However, when PA01 were suspended in CASO media they rapidly colonize the SAM, while poly(HPMA) and poly(MeOEGMA) brushes reduced the fouling close to the control values.

A much higher challenge was posed by the multi-resistance strain PA49. Massive fouling of these bacteria suspended in CASO (Figure 3, (3)) was observed on the SAM. While both poly(HPMA) and poly(MeOEGMA) brushes reduced the fouling by 30 and 15% compared to SAMs, these figures are much higher than for the other tested strains. This finding challenges the common practice of terming a surface as 'resistant to biofilm formation' when only one laboratory strain is tested.[65] Even if the prevention of the protein fouling leading to a conditioning film is a prerequisite to prevent the biofilm formation, the increase in the biofilm observed on PA49 clearly indicates that resistance to biofilm formation and biocompatibility are more complex than prevention of protein fouling as recently presented.[66] Arguably, the genetic variability of *P. aeruginosa* results in some strains able to colonize even surfaces fully resistant to protein adsorption, which lack the conditioning film. A feasible explanation for this phenomenon is the well know ability of this bacteria and next of its kind species to secrete extracellular polymeric substances (EPS), which may specifically interact with the studied brushes and promote adhesion or even by some specific interaction of protein or charged components of bacteria membrane with the surfaces.[67, 68] Thus, investigation on the mechanism of bacteria fouling should consider not only the physicochemical properties of the surface but the biological variability of the bacteria strains.

## Conclusions

In the current work, we report the resistance to bacteria fouling of ultra-low protein fouling polymer brushes based on poly(MeOEGMA) and poly(HPMA). Both brushes were prepared by surface-initiated atom transfer radical polymerization and characterized by FTIR, XPS, and water contact angle measurements.

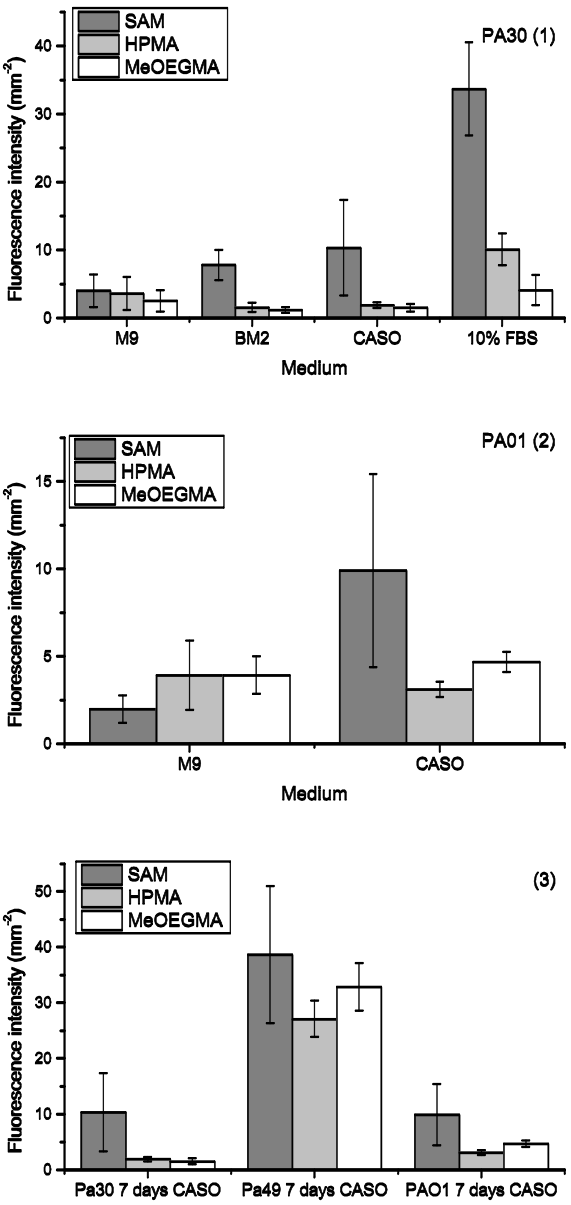


**Figure 3.** Fouling from different *P. aeruginosa* strains on SAM, poly(HPMA) and poly(MeOEGMA) brushes after 7 days contact. (1) environmental strain PA30 in different media, (2) PA01 in M9 and CASO and (3) comparative study of the fouling from PA30, PA49 and PA01 suspended in CASO.

The fluorescence intensity observed on both brushes after 7 days contact with PA30 suspended in low nutrient media (BM2 and M9) was below the controls, indicating no biofilm formation. An analogous experiment with protein and nutrient rich media CASO and 10% FBS resulted in no biofilm formation for the former and a decrease of the biofilm by 70% (poly(HPMA)) and 90% (poly(MeOEGMA)) for 10% FBS. The increase in fouling of the multi-resistant strain PA49 on



 

polymer brushes which fully prevent protein fouling, suggests that some strains are able to adhere to surfaces regardless of the formation of a conditioning film. Thus, more research on the genotypic and phenotypic variations of this bacterium is necessary for the design of surfaces resistant to even antibiotic multi-resistant bacteria. Both brush types showed an excellent resistance to biofilm formation even after 7 days of contact with *P. aeruginosa* (environmental and laboratory strains) in highly protein containing media such as 10% FBS. The remarkable resistance to biofilm formation and the possibility to precisely control their growth makes these brushes a promising candidate for surfaces of various biomaterials.

## Acknowledgements

C. R.-E. acknowledges support by the Alexander von Humboldt Foundation and the project BIOCEV – Biotechnology and Biomedicine Centre of the Academy of Sciences and Charles University (CZ.1.05/1.1.00/02.0109) from the European Regional Development Fund. F.S. and Z.S. acknowledge support of the Grant Agency of the Czech Republic under contract P106-12-1451. L.B., T.S. and C.B.-K. acknowledge funding from the Karlsruhe Institute of Technology (KIT) in the context of the BioInterfaces (BIF) program of the Helmholtz association. XPS was carried out with the support of the Karlsruhe Nano Micro Facility (KNMF), a Helmholtz Research Infrastructure at KIT.

## Notes and references

[1]Institute of Macromolecular Chemistry, Academy of Sciences of the Czech Republic, v.v.i., Heyrovsky sq. 2, 162 06 Prague, Czech Republic. E-mail: rodriguez@imc.cas.cz

[2] Preparative Macromolecular Chemistry, Institut für Technische Chemie und Polymerchemie, Karlsruhe Institute of Technology (KIT), Engesserstr. 18, 76128 Karlsruhe, Germany. E-mail: christopher.barner-kowollik@kit.edu.

[3] Soft Matter Synthesis Laboratory, Institut für Biologische Grenzflächen, KIT, Hermann-von-Helmholtz Platz 1, 76344 Eggenstein-Leopoldshafen, Germany. E-mail: leonie.barner@kit.edu.

[4] Institut für Funktionelle Grenzflächen, Karlsruhe Institute of Technology (KIT), Hermann-von-Helmholtz Platz 1, 76344 Eggenstein-Leopoldshafen, Germany.

† Electronic Supplementary Information (ESI) available: XPS, FT-IR and AFM measurements of the polymer brush surfaces, growth curves of three strains of *Pseudomonas* and protein fouling analysis via SPR. See DOI: 10.1039/x0xx00000x

1. S. J. Yuan, S. O. Pehkonen, Y. P. Ting, K. G. Neoh and E. T. Kang, *Langmuir*, 2010, **26**, 6728-6736.
2. P. Kingshott, J. Wei, D. Bagge-Ravn, N. Gadegaard and L. Gram, *Langmuir*, 2003, **19**, 6912-6921.
3. R. O. Darouiche, *N. Engl. J. Med.*, 2004, **350**, 1422-1429.
4. D. J. Stickler, *Curr. Opin. Infect. Dis.*, 2000, **13**, 389-393.
5. J. Hasan, R. J. Crawford and E. P. Ivanova, *Trends Biotechnol.*, 2013, **31**, 295-304.
6. R. O. Darouiche, *Clin. Infect. Dis.*, 1999, **29**, 1371-1377.
7. I. Banerjee, R. C. Pangule and R. S. Kane, *Adv. Mater.*, 2011, **23**, 690-718.
8. R. M. Klevens, J. R. Edwards, C. L. Richards Jr, T. C. Horan, R. P. Gaynes, D. A. Pollock and D. M. Cardo, *Public Health Rep.*, 2007, **122**, 160-166.
9. P. Gilbert, P. J. Collier and M. R. Brown, *Antimicrob. Agents Chemother.*, 1990, **34**, 1865-1868.
10. K. Vacheethasanee and R. E. Marchant, in *Handbook of Bacterial Adhesion: Principles, Methods, and Applications*, Humana Press, Totowa, NJ, 2000, pp. 73-90.
11. M. Y. Wu, V. Sendamangalam, Z. Xue and Y. Seo, *Biofouling*, 2012, **28**, 1119-1128.
12. B. Schachter, *Nat. Biotech.*, 2003, **21**, 361-365.
13. H. Ceri, M. E. Olson, C. Stremick, R. R. Read, D. Morck and A. Buret, *J. Clin. Microbiol.*, 1999, **37**, 1771-1776.
14. L. Timofeeva and N. Kleshcheva, *Appl. Microbiol. Biotechnol.*, 2011, **89**, 475-492.
15. C. Rodriguez-Emmenegger, M. Houska, A. B. Alles and E. Brynda, *Macromol. Biosci.*, 2012, **12**, 1413-1422.
16. C. Rodriguez-Emmenegger, E. Brynda, T. Riedel, M. Houska, V. Šubr, A. Bologna Alles, E. Hasan, J. E. Gautrot and W. T. S. Huck, *Macromol. Rapid Commun.*, 2011, **32**, 952–957.
17. C. Rodriguez-Emmenegger, E. Brynda, T. Riedel, Z. Sedlakova, M. Houska and A. B. Alles, *Langmuir*, 2009, **25**, 6328-6333.
18. A. Clements, F. Gaboriaud, J. F. Duval, J. L. Farn, A. W. Jenney, T. Lithgow, O. L. Wijburg, E. L. Hartland and R. A. Strugnell, *PLoS ONE*, 2008, **3**, e3817.
19. S. Gon and M. M. Santore, *Langmuir*, 2011, **27**, 15083-15091.
20. K. G. Neoh and E. T. Kang, *ACS Appl. Mater. Interfaces*, 2011, **3**, 2808-2819.
21. S. B. Lee, R. R. Koepsel, S. W. Morley, K. Matyjaszewski, Y. Sun and A. J. Russell, *Biomacromolecules*, 2004, **5**, 877-882.
22. F. J. Xu, K. G. Neoh and E. T. Kang, *Prog. Polym. Sci.*, 2009, **34**, 719-761.
23. E.-R. Kenawy, A. E.-R. R. El-Shanshoury, N. Omar Shaker, B. M. El-Sadek, A. H. B. Khattab and B. Ismail Badr, *J. Appl. Polym. Sci.*, 2011, **120**, 2734-2742.
24. T. Thorsteinsson, T. Loftsson and M. Masson, *Curr. Med. Chem.*, 2003, **10**, 1129-1136.
25. E.-R. Kenawy and Y. A. G. Mahmoud, *Macromol. Biosci.*, 2003, **3**, 107-116.
26. S. Gon, K.-N. Kumar, K. Nüsslein and M. M. Santore, *Macromolecules*, 2012, **45**, 8373-8381.
27. A. Roosjen, H. J. Busscher, W. Norde and H. C. van der Mei, *Microbiology*, 2006, **152**, 2673-2682.
28. F. Hui and C. Debiemme-Chouvy, *Biomacromolecules*, 2013, **14**, 585-601.
29. W. J. Yang, T. Cai, K. G. Neoh, E. T. Kang, G. H. Dickinson, S. L. Teo and D. Rittschof, *Langmuir*, 2011, **27**, 7065-7076.
30. R. Wang, K. G. Neoh, Z. Shi, E. T. Kang, P. A. Tambyah and E. Chiong, *Biotechnol. Bioeng.*, 2012, **109**, 336-345.
31. R. Hu, G. Li, Y. Jiang, Y. Zhang, J.-J. Zou, L. Wang and X. Zhang, *Langmuir*, 2013, **29**, 3773-3779.
32. Y. Wang, E. Y. Chi, D. O. Natvig, K. S. Schanze and D. G. Whitten, *ACS Appl. Mater. Interfaces*, 2013, **5**, 4555-4561.

33. G. Cheng, H. Xue, Z. Zhang, S. Chen and S. Jiang, *Angew. Chem. Int. Ed.*, 2008, **47**, 8831-8834.
34. A. Halperin, G. Fragneto, A. Schollier and M. Sferrazza, *Langmuir*, 2007, **23**, 10603-10617.
35. A. Halperin, *Langmuir*, 1999, **15**, 2525-2533.
36. A. Halperin and M. Kroger, *Langmuir*, 2012, **28**, 16623-16637.
37. H. J. Kaper, H. J. Busscher and W. Norde, *J. Biomater. Sci., Polym. Ed.*, 2003, **14**, 313-324.
38. F. Boulmedais, B. Frisch, O. Etienne, P. Lavalle, C. Picart, J. Ogier, J. C. Voegel, P. Schaaf and C. Egles, *Biomaterials*, 2004, **25**, 2003-2011.
39. E. Ostuni, R. G. Chapman, M. N. Liang, G. Meluleni, G. Pier, D. E. Ingber and G. M. Whitesides, *Langmuir*, 2001, **17**, 6336-6343.
40. B. Zdyrko, V. Klep and I. Luzinov, *Langmuir*, 2003, **19**, 10179-10187.
41. S. I. Jeon, J. H. Lee, J. D. Andrade and P. G. De Gennes, *J. Colloid Interface Sci.*, 1991, **142**, 149-158.
42. A. de los Santos Pereira, T. Riedel, E. Brynda and C. Rodriguez-Emmenegger, *Sensor Actuat. B- Chem.*, 2014, **202**, 1313-1321.
43. R. Advincula, *Adv. Polym. Sci.*, 2006, **197**, 107-136.
44. M. Zamfir, C. Rodriguez-Emmenegger, S. Bauer, L. Barner, A. Rosenhahn and C. Barner-Kowollik, *J. Mater. Chem. B*, 2013, **1**, 6027-6034.
45. T. Tischer, C. Rodriguez-Emmenegger, V. Trouillet, A. Welle, V. Schueler, J. O. Mueller, A. S. Goldmann, E. Brynda and C. Barner-Kowollik, *Adv. Mater.*, 2014, **26**, 4087-4092.
46. N. Y. Kostina, S. Sharifi, A. de los Santos Pereira, J. Michálek, D. W. Grijpma and C. Rodriguez-Emmenegger, *J. Mater. Chem. B*, 2013, **1**, 5644-5650.
47. O. Rzhepishevska, S. Hakobyan, R. Ruhal, J. Gautrot, D. Barbero and M. Ramstedt, *Biomater. Sci.*, 2013, **1**, 589-602.
48. V. L. Kung, E. A. Ozer and A. R. Hauser, *Microbiol. Mol. Biol. Rev.*, 2010, **74**, 621-641.
49. D. M. Jones, A. A. Brown and W. T. S. Huck, *Langmuir*, 2002, **18**, 1265-1269.
50. A. R. Kuzmyn, A. de los Santos Pereira, O. Pop-Georgievski, M. Bruns, E. Brynda and C. Rodriguez-Emmenegger, *Polym. Chem.*, 2014, **5**, 4124-4131.
51. K. L. Parry, A. G. Shard, R. D. Short, R. G. White, J. D. Whittle and A. Wright, *Surf. Interface Anal.*, 2006, **38**, 1497-1504.
52. J. H. Scofield, *J. Electron. Spectrosc. Relat. Phenom.*, 1976, **8**, 129-137.
53. S. Tanuma, C. J. Powell and D. R. Penn, *Surf. Interface Anal.*, 1994, **21**, 165-176.
54. C. K. Stover, X. Q. Pham, A. L. Erwin, S. D. Mizoguchi, P. Warrener, M. J. Hickey, F. S. L. Brinkman, W. O. Hufnagle, D. J. Kowalik, M. Lagrou, R. L. Garber, L. Goltry, E. Tolentino, S. Westbrock-Wadman, Y. Yuan, L. L. Brody, S. N. Coulter, K. R. Folger, A. Kas, K. Larbig, R. Lim, K. Smith, D. Spencer, G. K. S. Wong, Z. Wu, I. T. Paulsen, J. Reizer, M. H. Saier, R. E. W. Hancock, S. Lory and M. V. Olson, *Nature*, 2000, **406**, 959-964.
55. J. Li, T. Kleintschek, A. Rieder, Y. Cheng, T. Baumbach, U. Obst, T. Schwartz and P. A. Levkin, *ACS Appl. Mater. Interfaces*, 2013, **5**, 6704-6711.
56. N. Patenge, K. Arndt, T. Eggert, C. Zietz, B. Kreikemeyer, R. Bader, B. Nebe, V. Stranak, R. Hippler and A. Podbielski, *Biofouling*, 2012, **28**, 267-277.
57. A. de los Santos Pereira, C. Rodriguez-Emmenegger, F. Surman, T. Riedel, A. Bologna and E. Brynda, *R. Soc. Chem. Adv.*, 2014, **4**, 2318-2321.
58. C. Rodriguez-Emmenegger, E. Hasan, O. Pop-Georgievski, M. Houska, E. Brynda and A. Bologna Alles, *Macromol. Biosci.*, 2011, **12**, 525-532.
59. C. Rodriguez-Emmenegger, C. M. Preuss, B. Yameen, O. Pop-Georgievski, M. Bachmann, J. O. Mueller, M. Bruns, A. S. Goldmann, M. Bastmeyer and C. Barner-Kowollik, *Adv. Mater.*, 2013, **25**, 6123-6127.
60. C. M. Preuss, T. Tischer, C. Rodriguez-Emmenegger, M. M. Zieger, M. Bruns, A. S. Goldmann and C. Barner-Kowollik, *J. Mater. Chem. B*, 2014, **2**, 36-40.
61. Q. Yu, Y. Zhang, H. Wang, J. Brash and H. Chen, *Acta Biomater.*, 2011, **7**, 1550-1557.
62. G. B. Sigal, M. Mrksich and G. M. Whitesides, *J. Am. Chem. Soc.*, 1998, **120**, 3464-3473.
63. A. Kugel, S. Stafslien and B. J. Chisholm, *Prog. Org. Coat.*, 2011, **72**, 222-252.
64. A. K. Muszanska, E. T. J. Rochford, A. Gruszka, A. A. Bastian, H. J. Busscher, W. Norde, H. C. van der Mei and A. Herrmann, *Biomacromolecules*, 2014, **15**, 2019-2026.
65. G. Cheng, G. Li, H. Xue, S. Chen, J. D. Bryers and S. Jiang, *Biomaterials*, 2009, **30**, 5234-5240.
66. C. Blaszykowski, S. Sheikh and M. Thompson, *Trends Biotechnol.*, 2014, **32**, 61-62.
67. G. Hwang, S. Kang, M. G. El-Din and Y. Liu, *Biofouling*, 2012, **28**, 525-538.
68. O. Orgad, Y. Oren, S. L. Walker and M. Herzberg, *Biofouling*, 2011, **27**, 787-798.



 